Heat and Mass Transfer Research Journal
Vol. 2, No. 2; 2018
Published by CanSRG
http://cansrg.com/journals/hmtrj/

Experimental study of thermosyphon performance using R 407C

E. Z. Ibrahim[1], M. A. Halim[2], M. A. Omara[2] and W. Aziz[2,*]

[1]*Mechanical Department, Faculty of Engineering, Zagazig University, Egypt*
[2]*Mechanical Department, Faculty of Industrial Education, Suez University, Egypt*

Abstract

An experimental investigation was conducted to study the heat transfer performance of a two-phase closed thermosyphon for R 407C. The experiments show the effect of varying the heat flux, inclination angle and the filling ratio on the characteristics of the performance of thermothyphon. A copper tube of dimensions 1500 mm length and 25 mm inside diameter and 2 mm thickness is used as the thermosyphon, the selected heat flux varied from 1155 to 2853 W/m^2 and the selected filling ratios were 35, 50, 60 and 80 %. The thermosyphon inclination angle was changed from 0^o to 90^o at all filling ratios and heat fluxes. The experimental results proved that the inclination angle had an important effect on the thermal performance of the thermosyphon. The maximum heat transfer occurred at vertical inclination angle (θ = 90^o), and decreased as decreasing the inclination angle. The maximum performance of the thermosyphon value exists at a filling ratio of 50 % and inclination angle (θ = 90^o).

Keywords: *Two-phase thermosiphon; Filling ratio; Heat transfer; Inclination angle.*

Nomenclature

A	Surface area of the tube
c_P	Specific heat capacity
C_t	Overall heat transfer coefficient
d	Diameter of tube
	exit
g	Gravitational acceleration
h	Heat transfer coefficient
h_{fg}	Latent heat of vaporization
k	Thermal conductivity
K_p	Dimensionless parameter
L^+	The ratio of L_e/L_c
l_l	Film thickness scale
l_m	Bubble length scale
Nu	Nusselt number
P	pressure
Pr	Prandtl number
q	Heat flux
Ra	Rayleigh number
Re_g	Vapor Reynolds number
Re_{Le}	Reynolds number based on L_e
T	Temperature
V^+	Filling ratio
V_g	Mean vapor velocity at the evaporator
X	Dimensionless pool perimeter

Greek symbols

ρ	Density
μ	Dynamic viscosity
σ	Surface tension
α	Thermal diffusivity
β	Thermal expansion coefficient
ψ	Mixing pool coefficient
ν	kinematic viscosity

Subscripts

C	Condenser
E	Evaporator
G	Vapor
I	Inlet
L	Liquid
O	Outside
Oc	Outer surface of the condenser
Oe	Outer surface of the evaporator
S	Saturation

* Corresponding author
Submitted: July 8, 2018 Revised: September 17, 2018 Accepted: October 26, 2018

1. Introduction

Energy is a significant part of most daily base life. For this reason, the thermal execution of thermosyphon is an important part of the field of heat transfer. Thermosyphon needs small area, for this, the simplicity of design, high rate of heat transfer, less cost, less weight and less cost of repairs must be taken into consideration. A cross-section of a closed two-phase thermosyphon is shown in Figure 1. The thermosyphon consists of an evacuated sealed tube that contains a little amount of liquid. The useful heat in the evaporator section is conducted transversely across the pipe wall, causing the liquid in the thermosyphon to boil in the liquid pool region and evaporate or boil in the film region. In this technique, the working fluid absorbs the useful heat and converts it to latent heat. The vapor in the evaporator region is at a higher pressure than the condenser part causing the vapor to flow upward. In the condenser region, the vapor is condensed and thus releases the latent heat. The thermosyphon depends on gravity to force the liquid reverse to the evaporator section. Thermosyphons are considered self-actuated devices because no external power is needed for pumping the internal working fluid. The aim of present study is to investigate the thermal performance of a cooper, two-phase, closed thermosyphon, where R407 is the working fluid, for various inclination angles and different filling ratios.

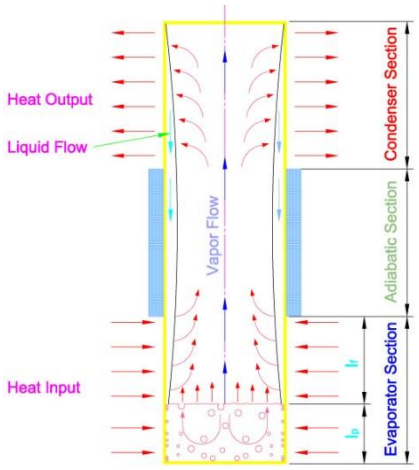

Figure 1. Two-phase closed thermosyphon working principle.

Chauhan et al. [1] introduced experimentally research of heat transfer increment techniques in closed Thermosyphon. The results indicated that the heat transfer efficiency is higher at coolant flow rate of 4 kg/h. Thermal performance of inclined thermosyphon with inclination angle of 90° is better for coolant flow rate of 4 kg/h. Karthikeyan et al. [2] used the aquatic solution of n-butanol to study heat transfer in closed thermosyphon. The results showed that the heat transfer coefficient of an aquatic solution of n-butanol is higher than that of the deionized water. Anjankar and Yarasu [3] perused experimental analysis of the effect of the condenser length on the performance of thermosyphon. The results were clear that the performance of 450 mm condensers length was higher than that of 400 mm and 350 mm condenser lengths for all flow rates. The results showed that the condenser section length should be 1.5 times of evaporator length to gain good thermal performance. Kannan et al. [4] studied the closed thermosyphon with various working fluids. The results concluded the maximum heat transport capability of water is high as compared to that of other working fluids like ethanol, methanol and acetone at all filling ratios and at all operating temperatures. In addition, the maximum heat transfer capability increases with increasing the operating temperature. Cho [5] studied the condensation heat transfer performance of condensers with internal fins and external plate fins of loop type two phases thermosyphon heat exchangers. The results illustrated that the heat transfer performance increased when the spaces between internal discontinuous pins decreased.

Gedik [6] studied the effect of various operating conditions on the thermal performance of two-phase closed thermosyphon. The results illustrated that the Ethylene glycol was a better-working fluid when the cooling water was 30 L/h. Ethanol was the best working fluid when the heat input was 600 W and the flow rates of the cooling water were 10 L/h. In addition, it was found that the inclination angle and heat input had significant effects on the efficiency of the two-phase closed thermosyphon (TPCT). Ashok and Mali [7] investigated the thermal Performance of thermosyphon heat pipe charged with binary mixture. The results showed that maximum heat transfer efficiency was 86.39% with 80^o inclination angle and 190 W heat load and. Binary mixture presentations showed a good thermal conductance of the thermosyphon heat pipe. Ong and Tong [8] studied the effect of inclination angle and water filling ratio on two-phase closed thermosyphon. The results explained the relationship between thermosyphon heat transfer and operating temperature. Kannan et al. [9] illustrated the heat transport capability of a two-phase thermosyphon charged with different working fluids. The results illustrated the maximum heat transport capability in water as compared to other fluids like ethanol methanol, and acetone at the operating temperatures higher than 40°C. Hammad and ALsuwaidi [10] illustrated the heat transfer coefficient of the thermosyphon cross-section shape. The results illustrated that the heat transfer coefficient increased by increasing the input power. Aruna V et al. [11] studied the flat plate type of solar water heater with a thermosyphon using different working fluid. The results showed that TiO2 with DI water gives the best performance when compared to propane. Oh et al. [12] illustrated the effect of fluid filling ratio on heat transfer properties of a two-phase closed thermosyphon. The results illustrated that the high heat transfer performance for the thermosyphon and effective thermal conductivity were obtained with a filling ratio of 40%.

2. Experimental apparatus

The experimental test device and test sections are illustrated in Figure 2 and Figure 3, respectively. The thermosyphon (1) is made of a smooth copper tube with an inside diameter of 25mm, thickness of 2mm and total length of 1500 mm that consists of three sections: adiabatic, evaporator, and condenser. The evaporator and condenser length is 600 mm and the adiabatic length is 300 mm. Perspex glass tube (water jacket) (6) surrounds the condenser section where the cooling water is flowing through the annular passage. The cooling water enters to the inner of the jacket from bottom section in a tangential direction to prevent thermosyphon from direct exposure to the water flow. A constant head tank (9) is placed 2000 mm above the head of the thermosyphon tube and is connected to the cooling section through a plastic tube. The make-up water provides the constant head tank through a float valve (8) to ensure that the water flow is nearly steady. There is also an overflow tube (14) that allows the exceeding water to flow to the drain. The flow rate of the cooling water is measured by a Rotameter (12). The main heater (24) of the evaporator section is made of a nickel-chrome strip (4.4 Ω/m, 3.1 mm wide and 0.2mm thick). The main heater is wrapped around the evaporator section at equal pitches (every 2mm of the evaporator length). Before wrapping the main heater, the bare smooth copper tube is wrapped with electrical insulating tape (23), which is made of a non-alkali fiberglass (0.13 mm thick and 25 mm wide). After winding the main heater, the main heater is wrapped with electrical insulating tape again. The main heater is covered by a cylindrical insulation (25). The insulation is made of glass wool (40 mm thick). The guard heater (26) is used to compensate for the heat loss from the main heater to the environment. The adiabatic section (21) is covered by glass wool insulation. For measuring the flat temperatures of the thermosyphon, 25 points of copper-constantan thermocouples (T-Type) of 1 mm diameter are used at 12 points in the evaporator section, 3 points in the adiabatic section, and 10 points for the condenser section) as shown in Figure 3. The thermocouples are embedded in slots and glued by a high conductive epoxy. The fluid temperatures are measured by using six thermocouples inserted inside the thermosyphon, where two thermocouples are press fitted into the thermosiphon sections as in Figure 3.

The inlet and outlet of cooling water were measured by Thermocouples T_{13} and T_{14}. All thermocouples are connected to a digital temperature recorder "Yokogawa" (19), which has an accuracy of ± 0.1 ^{o}C. Two autotransformers (17) are applied to control the power input to the main heater and the guard heater, individually. The power input to both the heater and the guard heater is calculated based on the values

measured by two analog ammeters (15) and two analog voltmeters (16) with an accuracy of ± 0.01A and ± 0.1V, respectively. Stabilizer (18) is connected with the two autotransformers to guarantee that input power fluctuations during the experimental run times are negligible.

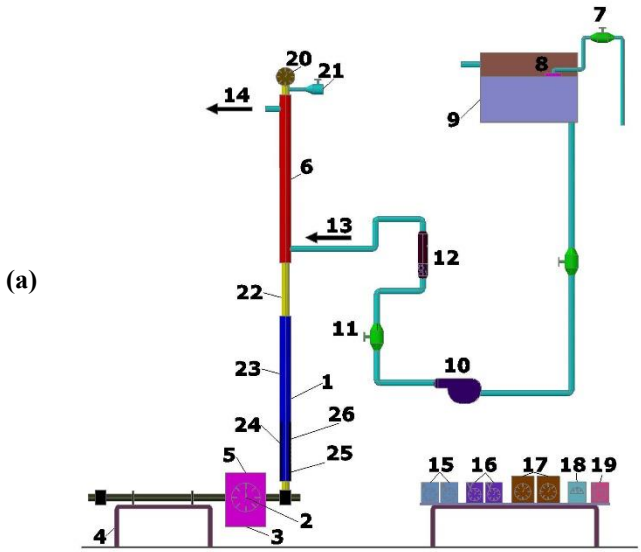

1- Thermosyphon
2- Pointer
3- Protractor
4- Base
5- Gear Box
6- Water jacket
7- Water Supply
8- Float valve
9- Constant head tank
10- Pump
11- Head valve
12- Rotameter
13- Water inlet
14- Water outlet
15- Ammeter
16- Voltmeter
17- Autotransformers
18- Stabilizer
19- temperature recorder

20- Pressure gauge
2l- Shut-off valve
22- Adiabatic section
23- Electric insulation
24- Main heater
25- Insulation
26- Guard heater.

Figure 2. Experimental setup: (a) experimental test rig, (b) experimental test section.

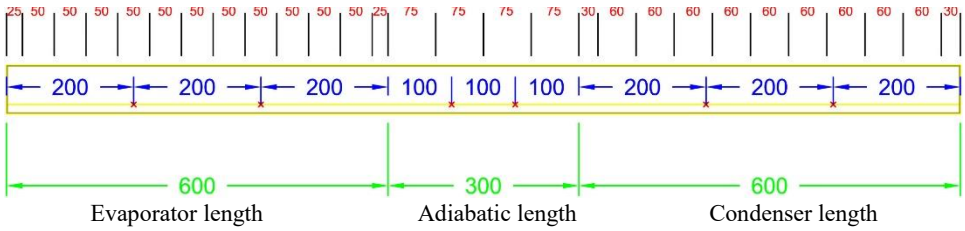

Figure 3. Details of thermocouples locations.

3. Data Reduction

There are a number of theoretical investigations in which film condensation heat transfer inside a thermosyphon has been studied with and without consideration of the counter-current vapor flow.

The heat transfer coefficient of the condenser obtained by

$$h_c = q_c / (t_s - t_{oc}) \quad (1)$$

where t_{oc} is the average outer wall temperature in the cooling zone and t_s as the saturation temperature in the vapor space.

Under steady state conditions, the heat transfer coefficient of the evaporator determined by

$$h_e = q_e / (t_{oe} - t_s) \quad (2)$$

where t_{oe} is the average outer surface temperature of the evaporator section wall and q_e is the input heat flux from the evaporator section that is given by

$$q_e = Q / A_e \quad (3)$$

The output heat flux in the condenser section is

$$q_c = Q / A_c \quad (4)$$

where Q is the input power and A_c and A_e are the area of the condenser and evaporator section, respectively.

The overall heat transfer execution of a heat pipe is generally characterized by the following equation introduced by Dunn [2]

$$C_t = Q / A_e (t_{oe} - t_{oc}) \quad (5)$$

or

$$C_t = 1 / (1/ h_e + L^+/ h_c) \quad (6)$$

where C_t is overall heat transfer coefficient and A_e is surface area of the evaporator. Thickness and velocity of the film grow to maximum values at the lower end of the cooling area. In the steady state, the working fluid inside the thermosyphon is in thermodynamic equilibrium with the saturation state at liquid level. The liquid below is subcooled to some value due to the hydrostatic pressure head, whereas the vapor does not deviate significantly from saturation. The liquid film Reynolds number at the exit of the evaporator is given as [13]

$$Re_{ext} = 4 Q / (\pi d_i \mu_l h_{fg}) \quad (7)$$

The liquid film Reynolds number founded on the evaporator length is given as

$$Re_{Le} = 4 q_e L_e /(\mu_l h_{fg}) \quad (8)$$

The mean vapor velocity at evaporator exit is given by the following expressions.

$$V_g = 4 q_e L_e / (\rho_g d_i h_{fg}) \quad (9)$$

Nusselt Number is calculated as

$$Nu = h_c l_l / k_l \quad (10)$$

where

$$l_l = [\mu_l^2 / (g \rho_l (\rho_l - \rho_g))]^{1/3} \quad (11)$$

The mixing coefficient, which reflects the contributions of mixing by sliding and altitude bubbles to the nucleate boiling heat transfer in the pool, is defined as

$$\psi = (\rho_g /\rho_l)^{0.4} [(p \nu_l / \sigma) (\rho_l^2 / (\sigma g (\rho_l - \rho_g))) ^{0.25}]^{0.25} \quad (12)$$

In the thermosyphon, there are three heat transfer regimes, which occur in small liquid pools in cylindrical enclosures, namely natural convection, combined convection and nucleate boiling. The different heat transfer modes are examined through employing a dimensionless parameter, X, which is defined [16] as

$$X = \psi Ra^{0.35} K_p^{0.7} Re_g^{0.7} Pr_l^{0.35} \quad (13)$$

$X < 10^6$ for natural convection, $X > 2.1\times 10^7$ for nucleate boiling and $10^6 < X < 2.1 \times 10^7$ in the

intermediate of combined convection, where

$$Ra = \beta\, g\, d_i^4\ q_e / K_l\ \nu_l\ \alpha_l\ K_p\ = P\ l_m / \sigma,$$

$$Pr_l = \mu_l\, C_p / k\ \ Re_g = q_e\ l_m / \rho_g\ \nu_l\ h_{fg},$$

$$\text{and}\ \ l_m\ = (\sigma / (g (\rho_l - \rho_g))) ^{0.25}$$

4. Results and discussion

4.1 Vertical position

The effect of different heat fluxes on the condenser and evaporator temperatures and operating temperature at different filling ratios (V^+) in vertical position ($\theta = 90^o$) are shown in Figure 4, Figure 5 and Figure 6. It is clear from these figures that when the heat flux increases, the temperatures of the evaporator and condenser and operation temperature increase at all values of filling ratios. This can be attributed to the rise of spatial pressure within the pool. This founding is in good agreement with [14].

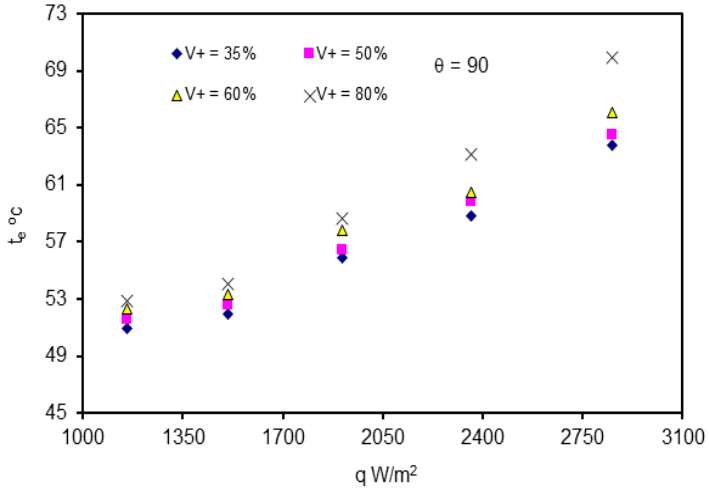

Figure 4. Effect of heat flux on the temperature of evaporator at different filling ratio with angle 90°.

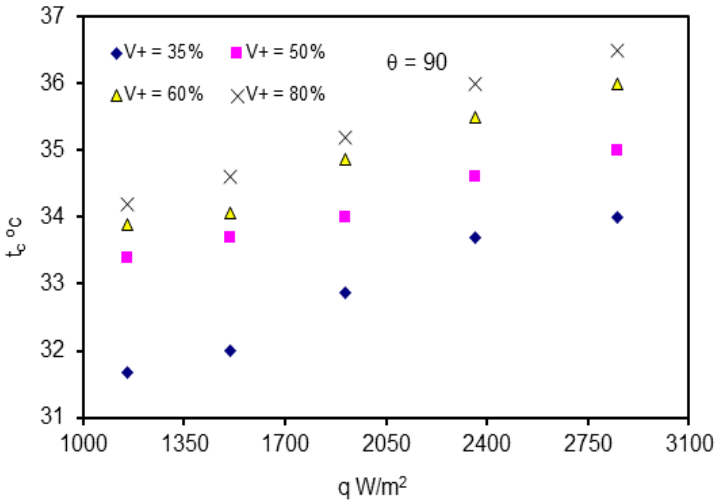

Figure 5. Effect of heat flux on the temperature of condenser at different filling ratio with angle 90°.

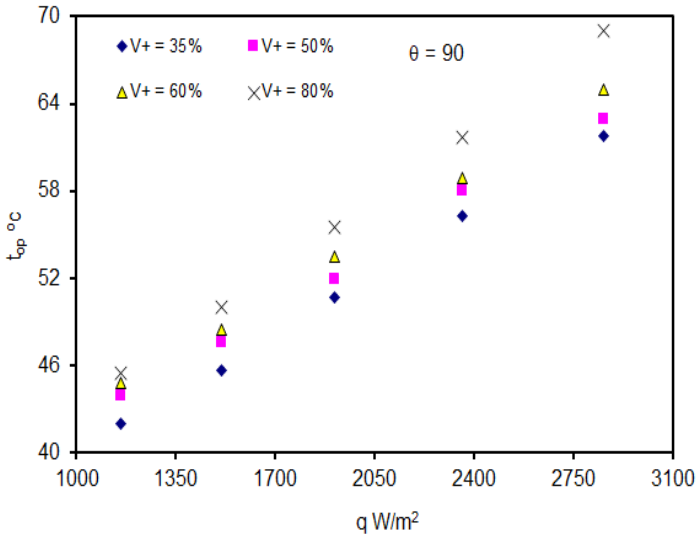

Figure 6. Effect of heat flux on the operating temperature at different filling ratio with angle 90°.

Figure 7 illustrates the variation of the evaporator and condenser temperature with filling ratios at constant heat flux. It is evident that the evaporator temperature increases than the condenser temperature. For example, at $V^+ = 0.5$, the evaporator-condenser temperature difference is about 22 °C at $q_e = 1687.6$ W/m^2. Figure 8 presents the relation between the heat transfer coefficient of the evaporator and the filling ratios (V^+) in a vertical position, the heat transfer coefficient of the evaporator section increases with heat fluxes for all filling ratios. The heat transfer coefficient of the condenser section (h_c) presents in figure 9 at various heat fluxes and filling ratios in a vertical position, this figure show that all data have the same trend, and the heat transfer coefficient of the condensation R407C decreases with increases the heat fluxes at all filling ratios, this is because very high circulate regime caused by rise the energy input, where the resistance of the produced film negative consequence on transforming heat from the evaporator to the condenser fluid. By additional heat to the evaporator a thick liquid layer founded in the condensation section causes higher thermal resistance.

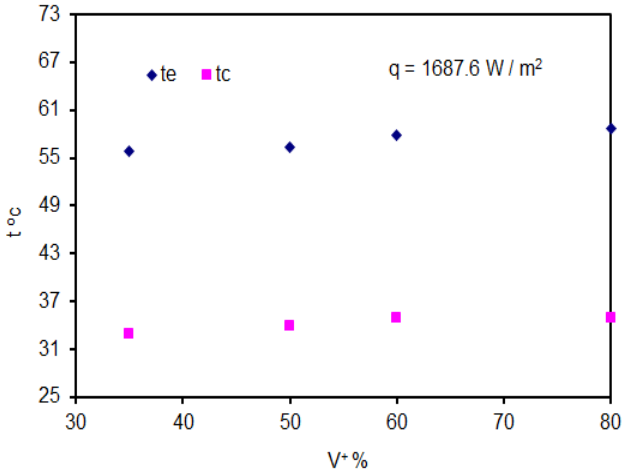

Figure 7. Effect of the thermosyphon filling ratio on the temperature of both evaporator and condenser at heat flux q = 1687.6 W/m^2.

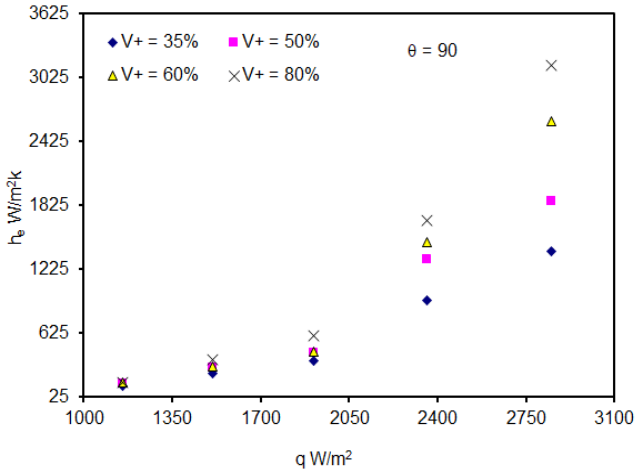

Figure 8. Effect of the heat flux on the heat transfer coefficient of evaporation at different filling ratio with angle 90°.

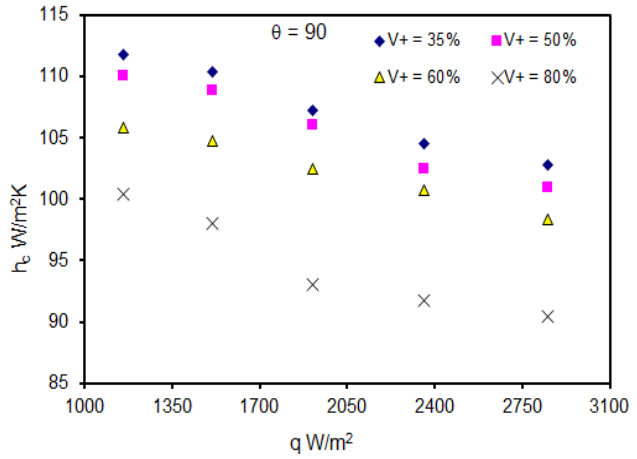

Figure 9. Effect of the heat flux on the heat transfer coefficient of condensation at different filling ratio with angle 90°.

The variation of filling ratios with the overall heat transfer coefficient at different heat fluxes in a vertical position, shows in figure 10. by increasing the filling ratio the overall heat transfer coefficient increase and reaches a maximum value at $V^+ = 0.5$, which clarified as "optimum filling ratio".

Then, the overall heat transfer coefficient decreases with increasing filling ratio and accomplish a minimum value at $V^+ = 0.8$ for all heat fluxes. This behavior explains the fact that the maximum performance of the thermosyphon takes place at $V^+ = 0.5$ at all heat fluxes when heat flux increase the overall heat transfer coefficient increases. This is because more bubbles generate with increasing heat fluxes then fly-up to the surface where they are converted to vapor, these bubbles raise the overall heat transfer coefficient.

The mixing pool coefficients Ψ reflects the sliding and rising bubbles to the nucleate boiling heat transfer in the pool. The mixing coefficients, depend on the physical properties of the working fluid, which increases by increasing vapor pressure, due to the increasing of mixing pool by vapor bubbles. Figure 11 presents the relation between the filling ratios and the mixing coefficient at

varying heat fluxes. In this figure, it is note increasing of mixing coefficient with rising the filling ratios and heat fluxes.

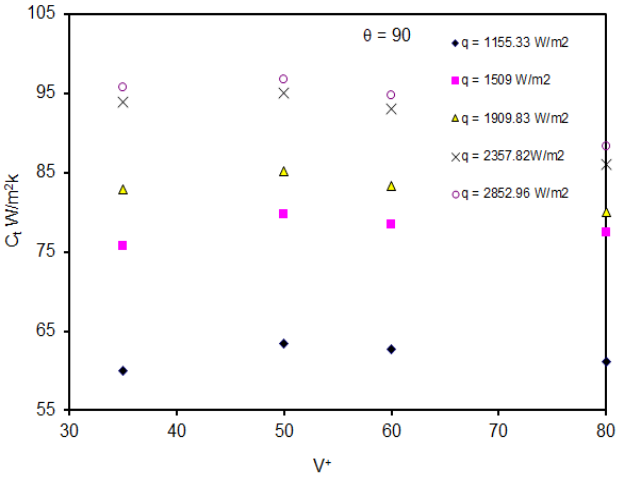

Figure 10. Effect of the filling ratio on the performance of thermosyphon at different heat flux with angle 90°.

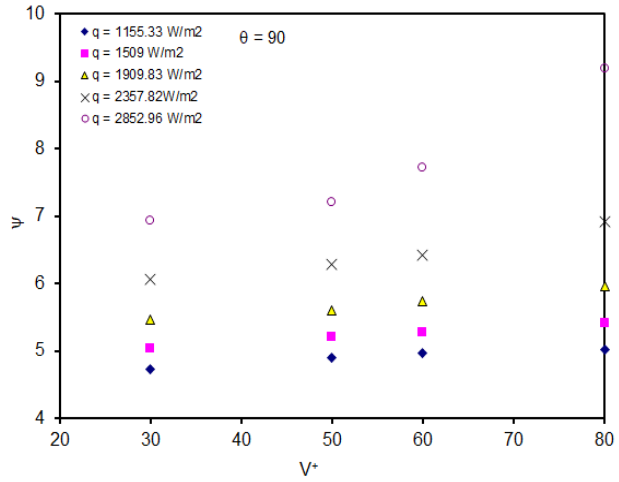

Figure 11. Effect of the thermosyphon filling ratio on the mixing pool coefficient at different heat flux with angle 90°.

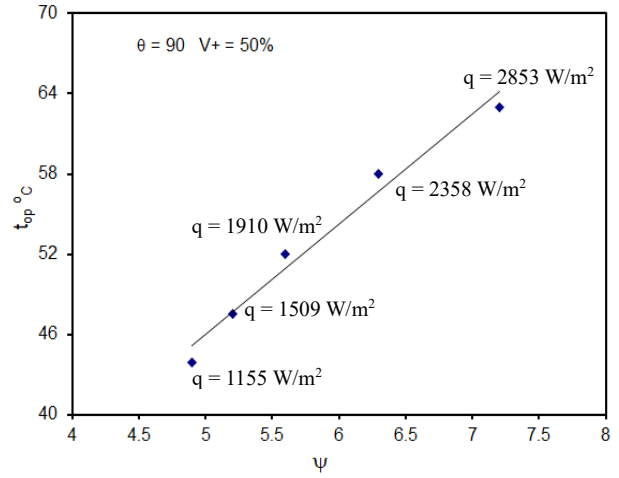

Figure 12. Effect of the mixing pool coefficient on the operating temperature at $v^{+} = 0.5$ with angle 90°.

The mixing coefficient and operating temperature with various heat fluxes at a constant filling ratio equal to 0.5, is explained in figure 12. The decreasing of the evaporator power decrease the vapor pressure and increases the latent heat of vaporization. This attributed to decrease the vapor generation rate and the mixing in the pool by departing and rising bubbles. For low latent heat of vaporization leading to rising vapor generation and mixing coefficient. Therefore, the enhancement of the nucleate boiling heat transfer as increasing the vapor temperature.

4.2 Inclined position

Figure 13 to figure16 illustrate the heat transfer coefficient of evaporator based on heat fluxes at varying inclination angles (60°, 75°and 90°) and filling ratios (35%, 50%, 60%, 80%) respectively. From these figures the heat transfer coefficients of the evaporator increase by increasing inclination angles at all filling ratios and heat fluxes. Means for vertical position of thermosiphon, the heat transfer efficiency is higher than the other inclinations. This is because at the lower inclination angles, heat transfer efficiency reduces due to the obstruction of vapour with the condensate return from the condenser. This obstruction causes heat transfer efficiency decreases between vapour and condensate.

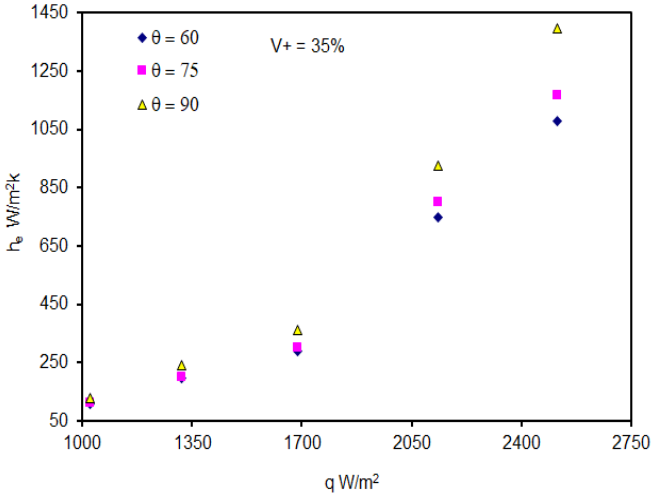

Figure 13. Effect of the heat flux on the heat transfer coefficient of evaporation at different angles with v^{+} = 0. 35.

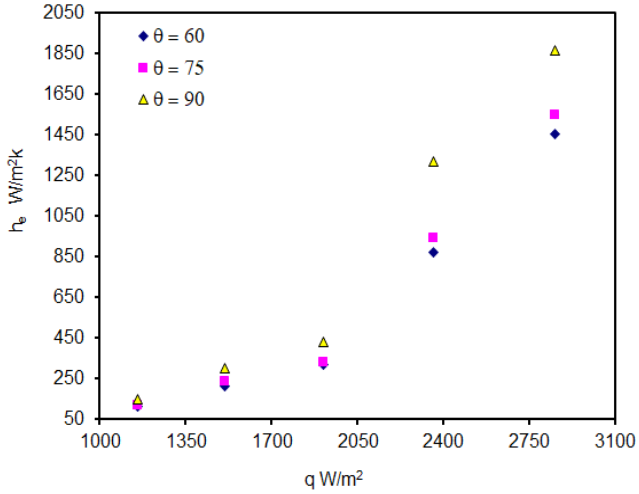

Figure 14. Effect of the heat flux on the heat transfer coefficient of evaporation at different angles with v^{+} = 0.5.

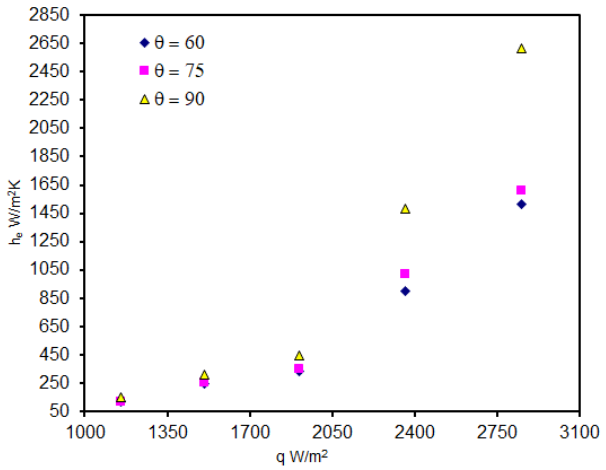

Figure 15. Effect of the heat flux on the heat transfer coefficient of evaporation at different angles with $v^+ = 0.6$.

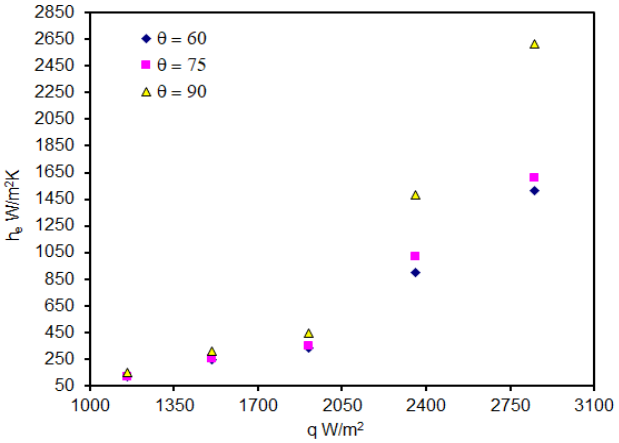

Figure 16. Effect of the heat flux on the heat transfer coefficient of evaporation at different angles with $v^+ = 0.8$.

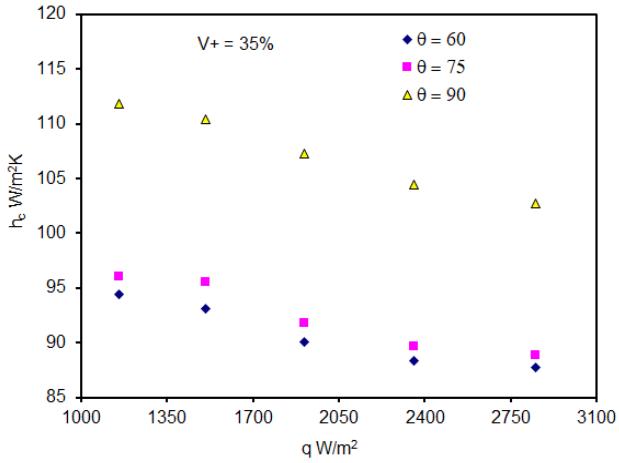

Figure 17. Effect of the heat flux on the heat transfer coefficient of condensation at different angles with $v^+ = 0.35$.

The heat transfer coefficient of condenser versus heat fluxes at varying inclination angles and constant filling ratio showing in figure 17 to figure 20. As shown in these figures, the maximum

condensation heat transfer coefficient decreases with increasing heat fluxes and take the same trend for all filling ratios. The maximum values of condensation heat transfer coefficient occurred at ($\theta = 90^o$), a thick liquid layer established in the condensation section by adding more heat to the evaporator. A higher thermal resistance refer to Increasing of thickness liquid layer and lower heat transfer coefficient then the capacity of heat absorption reduce.

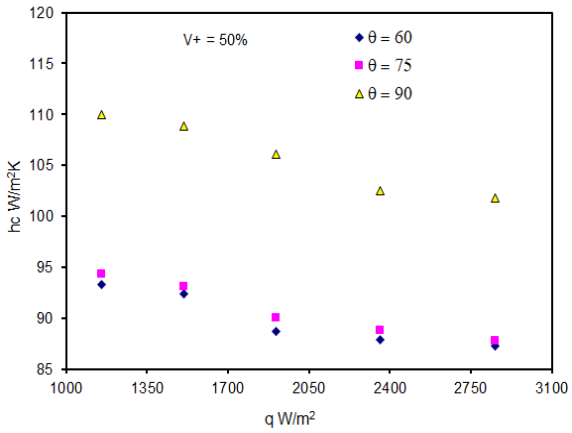

Figure 18. Effect of the heat flux on the heat transfer coefficient of condensation at different angles with $v^+ = 0.5$.

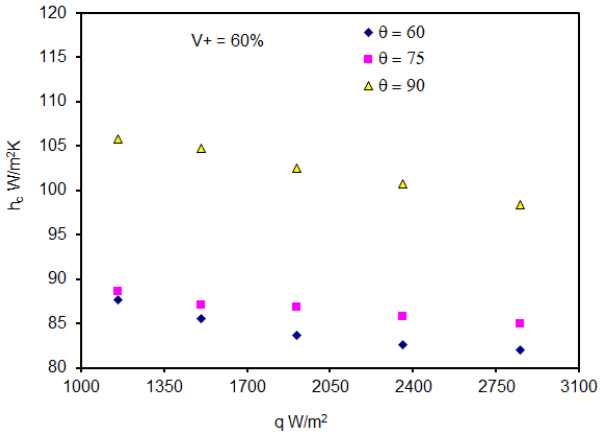

Figure 19. Effect of the heat flux on the heat transfer coefficient of condensation at different angles with $v^+ = 0.6$.

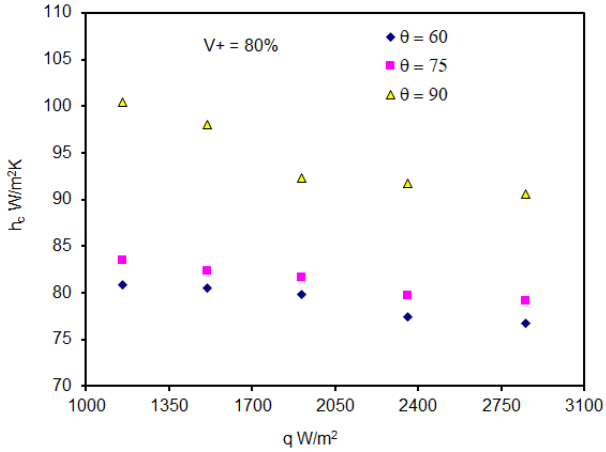

Figure 20. Effect of the heat flux on the heat transfer coefficient of condensation at different angles with $v^+ = 0.8$.

Figures 21 to 25 show the relation between the performances of the thermosyphon and different filling ratios at varying inclination angles and constant heat flux. The maximum values of performances of the thermosyphon at ($\theta = 90^o$), at any inclination angle the performance of the thermosyphon increases until arrive the maximum at filling ratio 50% and then decreases. This referred to the generated thick layers of vapor are attached to the wall at the bottom section, these thick vapor layers can cause a significant thermal resistance and decreasing the overall heat transfer.

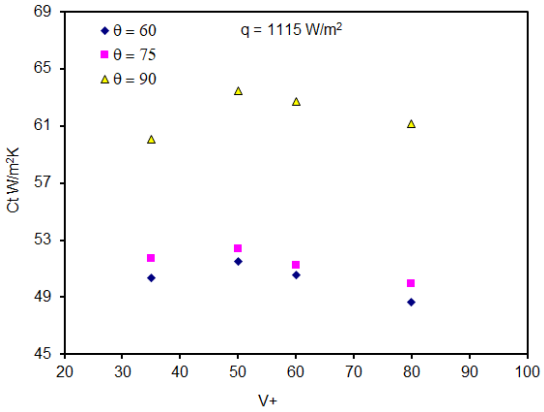

Figure 21. Effect of the filling ratio on the performance of thermosyphon at different angles with heat flux $q = 1115 W/m^2$.

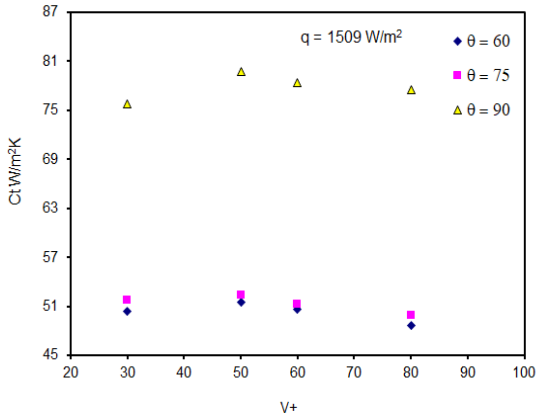

Figure 22. Effect of the filling ratio on the performance of thermosyphon at different angles with heat flux $q = 1509 W/m^2$.

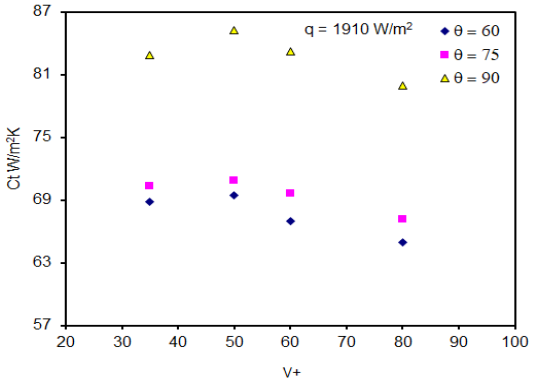

Figure 23. Effect of the filling ratio on the performance of thermosyphon at different angles with heat flux $q = 1910 W/m^2$.

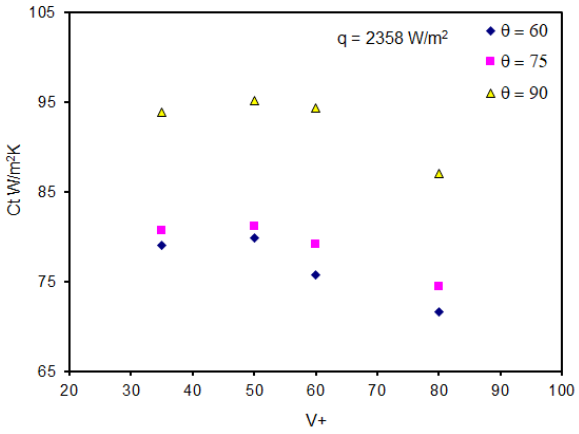

Figure 24. Effect of the filling ratio on the performance of thermosyphon at different angles with heat flux q = 2358 W/m^2.

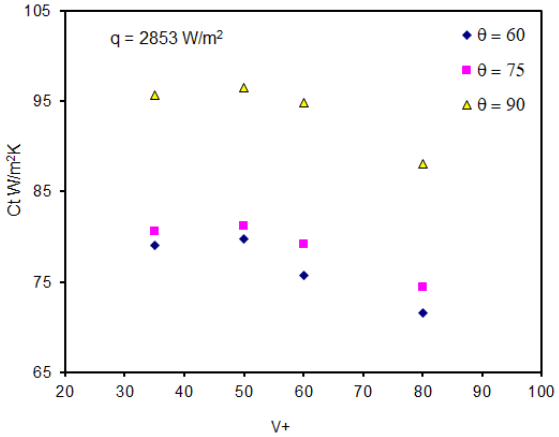

Figure 25. Effect of the filling ratio on the performance of thermosyphon at different angles with heat flux q = 2853 W/m^2.

5. Conclusions

The experimental investigation was carried out on thermosyphon charged with R 407C. The effect of filling ratio, heat flux and inclination angle on the performance of thermosyphon was experimentally investigated. Filling ratio was varied from 35% to 80% with inclination angle from 0^o to 90^o. The main results can be summarized as follows.

a- The thermosyphon wall temperatures, the operating temperature (corresponding to the operating pressure), the temperature difference between the evaporator and condenser, and the overall heat transfer coefficients are increased by increasing the input hat flux, over range of this study.

b- The boiling heat transfer coefficient is higher than the condensation heat transfer coefficient.

c- The maximum performance of the thermosyphon by using R407C is obtained at the filling ratio of 50%, therefore, this value is called optimum filling ratio.

d- Thermal performance of inclined thermosyphon with inclination angle 90° is better. This is because at vertical position condensate returns to evaporator at fast rate and there is restriction to appears flooding as well as entrainment limit.

e- The mixing coefficient, increases with increasing vapor pressure or temperature of the vapor due to increased mixing in the pool by vapor bubbles.

f- Increasing the vapor temperature or vapor pressure by increasing the power throughput would be enhancing the nucleate boiling heat transfer.

References

[1] Sandipkumar B. Chauhan, M. Basavaraj and Prashant Walke, Experimental investigation of heat transfer enhancement techniques in two phase closed thermosyphon, International Journal of Engineering Research and General Science, vol 4(2), 2016.

[2] M. Karthikeyan, S. Vaidyanathan and B. Sivaraman, Heat transfer analysis of two phase closed thermosyphon using aqueous solution of n-Butanol, International Journal of Engineering and Technology, vol 3(6), 2013.

[3] P. G. Anjankar and R. B. Yarasu, Experimental analysis of condenser length effect on the performance of thermosyphon, International Journal of Emerging Technology and Advanced Engineering, vol 2(3), 2012.

[4] M. Kannan, J. Murugan1, B. Deepanraj and A. Santhoshkumar, Thermal performance of a two phase closed thermosyphon charged with different working fluids, Daffodil International University Journal of Science and Technology, vol 9(1), 2014.

[5] Dong-Hyun Cho, A study on the condensation heat transfer performance of condensers with internal fins and external plate fins of loop type two phases thermosyphon heat exchangers, Advanced Science and Technology Letters, vol.120, pp. 701-707, 2015.

[6] Engin Gedik, Experimental investigation of the thermal performance of a two-phase closed thermosyphon at different operating conditions, Energy and Buildings, vol 127, pp. 1096-1107, 2016.

[7] Faddas Nikhil Ashok and K. V. Mali, Thermal performance of thermosyphon heat pipe charged with binary mixture, International Journal of Science, Engineering and Technology Research (IJSETR), volume 4(1), pp. 92 -102, 2015.

[8] K. S. Ong and W. L. Tong, Inclination and fill ratio effects on water filled two-phase closed thermosyphon, 10th IHPS, Taipei, Taiwan, Nov. 6-9, 2011.

[9] M. Kannan, R. Senthil, R. Baskaran and B. Deepanraj, An experimental study on heat transport capability of a two phase thermosyphon charged with different working fluids, American Journal of Applied Sciences, vol 11(4), pp. 584-591, 2014.

[10] Mohammed M. I. Hammad and Jasem H. ALsuwaidi, Experimental investigation on the heat transfer coefficient of the thermosyphon cross section shape, Journal of Engineering Research and Applications, vol. 5(3), pp. 57-66, 2015.

[11] Aruna V, Dr. Channakaiah and G. Murali, A study on a flat plate type of solar water heater with an thermosyphon using different working fluid, International Journal of Engineering Trends and Technology, vol 22(10), pp. 493-497, 2015.

[12] S. H. Oh, S. I. Kim, J. W. Choi, K. J. Lee and W. P. Chun, Heat transfer characteristics of a two-phase closed thermosyphon considering the working fluid filling ratio, Korea Institute of Energy Research, 14th International Conference on Simulation and Experiments in Heat Transfer and its Applications, Korea, 2016.

[13] Hamed H. Saber, Operation envelope and performance analyses of closed two-phase thermosyphons, Ph.D. Thesis, New Mexico University, New Mexico, USA, 2000.

[14] M. S. Saadawy, Study of the performance of a liquid metal high temperature heat pipe, Ph.D. Thesis, Ain-Shams University, Cario, Egypt, 1996.